

Diamidodipyrins: Versatile Bipyrrolic Ligands with Multiple Metal Binding Modes

Van S. Thoi,[†] Jay R. Stork,[†] Edwards T. Niles,[‡] Ezra C. Depperman,[‡] David L. Tierney,^{*‡} and Seth M. Cohen^{*†}

Department of Chemistry and Biochemistry, University of California, San Diego, 9500 Gilman Drive, La Jolla, California 92093-0358, and Department of Chemistry and Chemical Biology, University of New Mexico, Albuquerque, New Mexico 87131

Received June 27, 2008

A straightforward, facile synthesis of diamidodipyrromethenes (diamidodipyrins, DADP^{R,R'}) is presented. These tetradentate ligands readily form complexes with metal ions such as Ni²⁺ and Cu²⁺ and can adopt different binding modes with these metals. One version of the ligand (DADP^{Ph,Pr}) has been structurally characterized in its “free base” form, as a HBr salt, and as the Ni²⁺ and Cu²⁺ complexes. A symmetric NNOO donor set is found for the Cu²⁺ complex in the solid state, involving two carbonyl oxygen atoms and two dipyrin nitrogen atoms, and this coordination mode has been confirmed in solution by electron paramagnetic resonance. An asymmetric NNNO binding mode found for the Ni²⁺ complex in the solid state persists in solution as revealed by ¹H NMR. The HBr salt form of the ligand shows an intriguing hydrogen-bonded head-to-head dimer arrangement. Experiments show that Cu²⁺, but not Ni²⁺, can mediate the rapid oxidation of the diamidodipyrromethane precursors to the diamidodipyrromethene ligands in the presence of dioxygen. The work here shows that diamidodipyrins are a versatile new class of ligands in the area of nonporphyrinic pyrrole-based compounds that merit further investigation.

Introduction

Studies into the coordination chemistry of nonporphyrinic, pyrrole-based ligands have formed an area of great interest in coordination chemistry.^{1–8} Among these ligands, the dipyrins (dipyrromethenes) have been heavily studied, with

numerous metal complexes reported.⁹ Dipyrinato metal complexes that have been described in the literature include fluorescent complexes (with Zn²⁺, Ga³⁺, and In³⁺),^{10,11} incorporation into discrete supramolecular structures,^{6,12,13} and use as metalloligands for coordination polymers and metal-organic frameworks.^{14–17} Perhaps the most well-known dipyrinato derivatives are the BODIPY dyes,^{18,19}

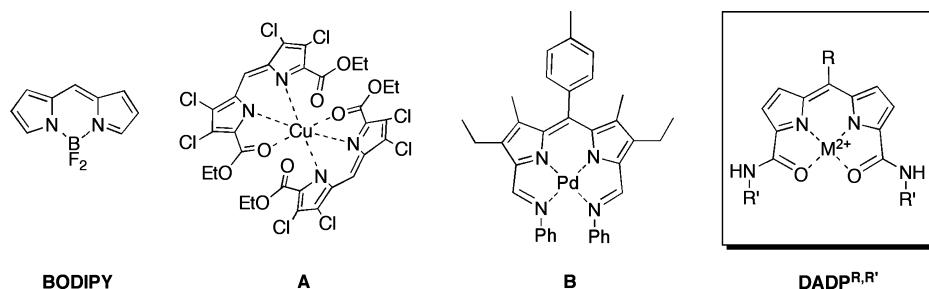
* Authors to whom correspondence should be addressed. Telephone: (858) 822-5596(S.M.C.), (505) 277-2505(D.L.T.). Fax: (858) 822-5598 (S.M.C.), (505) 277-2609 (D.L.T.). E-mail: scohen@ucsd.edu (S.M.C.), dtierney@unm.edu (D.L.T.).

[†] University of California.

[‡] University of New Mexico.

- (1) Wampler, K. M.; Schrock, R. R. *Inorg. Chem.* **2007**, *46*, 8463–8465.
- (2) Bachmann, J.; Nocera, D. G. *J. Am. Chem. Soc.* **2005**, *127*, 4730–4743.
- (3) Katayev, E. A.; Severin, K.; Scopelliti, R.; Ustynyuk, Y. A. *Inorg. Chem.* **2007**, *46*, 5465–5467.
- (4) Shi, Y. H.; Cao, C. S.; Odom, A. L. *Inorg. Chem.* **2004**, *43*, 275–281.
- (5) Givajja, G.; Volpe, M.; Edwards, M. A.; Blake, A. J.; Wilson, C.; Schroder, M.; Love, J. B. *Angew. Chem., Int. Ed.* **2007**, *46*, 584–586.
- (6) Wood, T. E.; Dagleish, N. D.; Power, E. D.; Thompson, A.; Chen, X.; Okamoto, Y. *J. Am. Chem. Soc.* **2005**, *127*, 5740–5741.
- (7) Sessler, J. L.; Tomat, E.; Lynch, V. M. *J. Am. Chem. Soc.* **2006**, *128*, 4184–4185.
- (8) Harman, W. H.; Chang, C. J. *J. Am. Chem. Soc.* **2007**, *129*, 15128–15129.

- (9) Wood, T. E.; Thompson, A. *Chem. Rev.* **2007**, *107*, 1831–1861.
- (10) Sazanovich, I. V.; Kirmaier, C.; Hindin, E.; Yu, L.; Bocian, D. F.; Lindsey, J. S.; Holten, D. *J. Am. Chem. Soc.* **2004**, *126*, 2664–2665.
- (11) Thoi, V. S.; Stork, J. R.; Magde, D.; Cohen, S. M. *Inorg. Chem.* **2006**, *45*, 10688–10697.
- (12) Zhang, Y.; Thompson, A.; Rettig, S. J.; Dolphin, D. *J. Am. Chem. Soc.* **1998**, *120*, 13537–13538.
- (13) Thompson, A.; Rettig, S. J.; Dolphin, D. *Chem. Commun.* **1999**, 631–632.
- (14) Gill, H. S.; Finger, I.; Bozidarevic, I.; Szydlo, F.; Scott, M. J. *New J. Chem.* **2005**, *29*, 68–71.
- (15) Halper, S. R.; Cohen, S. M. *Inorg. Chem.* **2005**, *44*, 486–488.
- (16) Halper, S. R.; Do, L.; Stork, J. R.; Cohen, S. M. *J. Am. Chem. Soc.* **2006**, *128*, 15255–15268.
- (17) Halper, S. R.; Malachowski, M. R.; Delaney, H. M.; Cohen, S. M. *Inorg. Chem.* **2004**, *43*, 1242–1249.
- (18) Loudet, A.; Burgess, K. *Chem. Rev.* **2007**, *107*, 4891–4932.
- (19) Kim, H.; Burghart, A.; Welch, M. B.; Reibenspies, J.; Burgess, K. *Chem. Commun.* **1999**, 1889–1890.

Chart 1. Some Dipyrin Complexes Described in the Literature and the Diamidodipyrin (DADP^{R,R'}) Complexes Presented Herein (Right, in Box)

which are boron (often boron difluoride, Chart 1) adducts that display rich optical properties including robust photoluminescence.

Historically, only a few examples of dipyrin ligands with additional ligating groups in the α position of the pyrroles have been described. Martell et al. utilized 3,3',4,4'-tetrachloro-5,5'-diethoxycarbonyldipyrromethene (Chart 1, A),^{20,21} which contains both nitrogen and oxygen donors, as ligands for Co²⁺, Ni²⁺, Cu²⁺, and Zn²⁺ ions.²¹ The Co²⁺ and Zn²⁺ complexes were reported to have nearly tetrahedral coordination geometries, based on IR spectroscopy, from which the authors concluded that an ML₂ complex, with four pyrrolic nitrogen atoms from two dipyrin ligands, was formed. The same study presented X-ray diffraction and electron paramagnetic resonance (EPR) data of the Ni²⁺ and Cu²⁺ complexes that suggested a distorted octahedral coordination sphere; it was concluded that these metals were coordinated to two ligands via two pyrrolic nitrogen atoms and one oxygen atom from each ligand. Unfortunately, these structural assignments were not confirmed with single-crystal X-ray diffraction experiments.

More recently, a greater variety of α -substituted dipyrromethane and dipyrromethene ligands have been investigated for their anion^{22,23} and metal-binding properties. Love and co-workers have reported a number of interesting systems based on α -substituted dipyrromethane ligands.^{5,24,25} Diamidopyridine–dipyrromethane hybrid macrocycles have been reported to coordinate to Pd²⁺ through pyrrolic and imino nitrogen atoms.²⁶ The synthesis of diiminodipyrromethane and diiminodipyrromethene complexes of Ni²⁺, Pd²⁺, and Pt²⁺ has also been described.³ These complexes use a NNNN donor set, comprised of two pyrrolic and two imino nitrogen atoms, to chelate to the metal (Chart 1, B). Interestingly, these diiminodipyrromethane complexes react with dioxygen and oxidize to form a variety of α -substituted

dipyrin complexes with NNNN and NNNO donor atoms. These new studies strongly suggested that related α -substituted dipyrins, namely, diamidodipyrins, should display rich coordination chemistry. Although diiminodipyrins, dicarbonyldipyrins, and their metal complexes have been described, the use of diamidodipyrin ligands has not been widely explored. The present report describes a general, high-yielding synthesis of diamidodipyrins, as well as their complexes with Ni²⁺ and Cu²⁺. Diamidodipyrins are found to form 1:1 metal–ligand complexes with either a four- or five-coordinate geometry. Furthermore, the diamidodipyrin can serve as a NNOO or NNNO donor depending on the metal ion bound.

Experimental Section

General. Unless otherwise noted, starting materials were obtained from commercial suppliers and used without further purification. Mass spectrometry was performed at the University of California, San Diego Mass Spectrometry Facility in the Department of Chemistry and Biochemistry. A ThermoFinnigan LCQ-DECA mass spectrometer was used for electrospray ionization (ESI) or atmospheric pressure chemical ionization analysis, and the data were analyzed using the Xcalibur software suite. Elemental analysis was performed at NuMega Resonance Laboratories, San Diego, California. ¹H/¹³C NMR spectra were recorded on Varian FT-NMR spectrometers at the Department of Chemistry and Biochemistry, University of California, San Diego. UV–visible absorption spectra were recorded using a Perkin-Elmer Lambda 25 spectrophotometer with the UVWinLab 4.2.0.0230 software package. Absorbance spectra are reported as λ_{\max}/nm ($\epsilon/\text{M}^{-1} \text{cm}^{-1}$).

N-Isopropyl-1H-pyrrole-2-carboxamide (1a). Trichloroacetylpyrrole (5.0 g, 24 mmol) was added to 50 mL of isopropylamine, and the mixture was stirred at room temperature. The originally clear solution became light brown. After 17 h, the solvent was removed with a rotary evaporator to yield an off-white precipitate (3.4 g, 22 mmol, 94%). ¹H NMR (400 MHz, DMSO-*d*₆): δ 11.37 (s, 1H), 7.70 (d, *J* = 8.1 Hz, 1H), 6.81 (d, *J* = 4.4 Hz, 1H), 6.76 (d, *J* = 5.9 Hz, 1H), 6.05 (s, 1H), 4.04 (m, 1H), 1.13 (d, *J* = 6.6 Hz, 6H). ¹³C NMR (CDCl₃): δ 160.8, 121.7, 109.7, 94.5, 41.6, 23.2. ESI-MS: *m/z* 153.10 [M + H]⁺.

[1,1'-Isopropylamide-5-phenyl-4,6-dipyrromethane] (2a). To a solution of **1a** (1.0 g, 6.5 mmol) suspended in 30 mL of toluene was added benzaldehyde (0.33 g, 3.2 mmol) and *p*-toluenesulfonic acid (*p*-TSA, ~5 mg), and the resulting solution was heated to 120 °C. After 16 h, a pink precipitate was filtered and washed with 60 mL of toluene (1.0 g, 2.5 mmol, 78%). ¹H NMR (400 MHz, DMSO-*d*₆): δ 11.25 (s, 2H), 7.63 (d, *J* = 8.1 Hz, 2H), 7.28–7.11 (m, 5H), 6.65 (d, *J* = 3.7 Hz, 2H), 5.74 (d, *J* = 3.7 Hz, 2H), 5.48 (s, 1H),

(20) Motekaitis, R. J.; Martell, A. E. *Inorg. Chem.* **1970**, *9*, 1832–1839.

(21) Murakami, Y.; Matsuda, Y.; Sakata, K.; Martell, A. E. *Dalton Trans.* **1973**, 1729–1734.

(22) Vega, I. E.; Gale, P. A.; Hursthouse, M. B.; Light, M. E. *Org. Biomol. Chem.* **2004**, *2*, 2935–2941.

(23) Katayev, E. A.; Boev, N. V.; Khrustalev, V. N.; Ustynyuk, Y. A.; Tananaev, I. G.; Sessler, J. L. *J. Org. Chem.* **2007**, *72*, 2886–2896.

(24) Givaja, G.; Volpe, M.; Leeland, J. W.; Edwards, M. A.; Young, T. K.; Darby, S. B.; Reid, S. D.; Blake, A. J.; Wilson, C.; Wolowska, J.; McInnes, E. J. L.; Schroder, M.; Love, J. B. *Chem.—Eur. J.* **2007**, *13*, 3707–3723.

(25) Reid, S. D.; Blake, A. J.; Kockenberger, W.; Wilson, C.; Love, J. B. *Dalton Trans.* **2003**, 4387–4388.

(26) Katayev, E. A.; Ustynyuk, Y. A.; Lynch, V. M.; Sessler, J. L. *Chem. Commun.* **2006**, 4682–4684.

4.00 (m, 2H), 1.07 (d, $J = 6.6$ Hz, 12H). ^{13}C NMR (DMSO- d_6): δ 160.4, 143.2, 137.0, 128.8, 127.0, 126.6, 126.2, 110.7, 108.3, 43.4, 23.3. ESI-MS: m/z 393.08 [M + H] $^+$, 415.17 [M + Na] $^+$.

[1,1'-Isopropylamide-5-phenyl-4,6-dipyrin] (HDADP^{Ph,Pr}). A solution of 2,3-dicyano-5,6-dichloro-1,4-benzoquinone (DDQ, 0.13 g, 0.59 mmol) in 25 mL of tetrahydrofuran (THF) was added dropwise to a solution of **2a** (0.20 g, 0.51 mmol) suspended in 50 mL of THF and 30 mL of CHCl_3 over 15 min. Upon addition, the solution became a turbid, orange mixture, and after 23 h, the solution was dark red. The solvent was removed with a rotary evaporator, and the residue was purified by flash chromatography on a silica gel column (CH_2Cl_2). A red band was isolated and yielded a bright orange product (0.18 g, 0.47 mmol, 93%). ^1H NMR (400 MHz, CDCl_3): δ 7.48 (m, 5H), 6.77 (d, $J = 4.4$ Hz, 2H), 6.63 (d, $J = 4.4$ Hz, 2H), 6.55 (d, $J = 8.1$ Hz, 2H), 4.29 (m, 2H), 1.32 (d, $J = 6.6$ Hz, 12H). ^{13}C NMR (CDCl_3): δ 160.3, 149.4, 144.7, 142.0, 136.5, 131.2, 130.3, 129.9, 128.1, 117.2, 41.9, 23.0. ESI-MS: m/z 319.17 [M + H] $^+$. λ_{max} (15% $\text{CH}_3\text{OH}/\text{CH}_2\text{Cl}_2$): 456 (15000), 334 (5600). Anal. calcd for $\text{C}_{23}\text{H}_{26}\text{N}_4\text{O}_2 \cdot \text{H}_2\text{O}$: C, 67.63; H, 6.91; N, 13.72. Found: C, 67.55; H, 7.01; N, 13.70.

N-Cyclohexyl-1H-pyrrole-2-carboxamide (1b). Trichloroacetylpyrrole (3.0 g, 14 mmol) was added to 10 mL of cyclohexylamine, and the mixture was stirred at room temperature. The mixture became a turbid suspension with a white precipitate overnight. The white precipitate was filtered and washed with 40 mL of Et_2O (1.3 g, 6.8 mmol, 48%). ^1H NMR (500 MHz, CDCl_3): δ 9.60 (s, 1H), 6.90 (s, 1H), 6.51 (s, 1H), 6.218 (d, $J = 5.8$ Hz, 1H), 5.72 (d, $J = 6.8$ Hz, 1H), 3.93 (m, 1H), 2.02–1.16 (m, 10H). ^{13}C NMR (DMSO- d_6): δ 160.3, 127.2, 121.6, 110.4, 109.0, 48.1, 33.4, 26.0, 25.7. ESI-MS: m/z 193.22 [M + H] $^+$.

[1,1'-Cyclohexylamide-5-phenyl-4,6-dipyrromethane] (2b). To a suspension of **1b** (0.80 g, 4.2 mmol) in 30 mL of toluene was added benzaldehyde (0.22 g, 2.1 mmol) and *p*-TSA (~5 mg). The mixture became transparent pink upon heating to 120 °C. After heating overnight, a pink precipitate formed, which was filtered and washed with 70 mL of toluene (0.80 g, 1.6 mmol, 82%). ^1H NMR (400 MHz, DMSO- d_6): δ 11.26 (s, 2H), 7.62 (s, 2H), 7.30–7.12 (m, 5H), 6.68 (q, $J = 5.8$ Hz, 2H), 5.74 (q, $J = 5.8$ Hz, 2H), 5.50 (s, 1H), 3.68 (m, 2H), 1.78–1.11 (m, 10H). ^{13}C (DMSO- d_6): δ 160.3, 143.2, 137.0, 129.6, 128.8, 126.5, 110.8, 108.3, 48.1, 33.4, 26.0, 25.7. ESI-MS: m/z 473.23 [M + H] $^+$, 495.34 [M + Na] $^+$.

[1,1'-Cyclohexylamide-5-phenyl-4,6-dipyrin] (HDADP^{Ph,Cy}). A solution of DDQ (0.16 g, 0.70 mmol) in 30 mL of THF was added dropwise to a solution of **2b** (0.22 g, 0.47 mmol) in 50 mL of CHCl_3 over 15 min. Upon addition, the solution became red and transparent. After 5 h, the reaction was complete by thin-layer chromatography (TLC), and the solvent was removed on a rotary evaporator. The residue was purified by flash chromatography on a silica gel column (CH_2Cl_2), and a red band was isolated. The product was chromatographed on a second silica gel column in CH_2Cl_2 with 3% MeOH, yielding a red film (0.20 g, 0.4 mmol, 91%). ^1H NMR (400 MHz, CDCl_3): δ 7.52–7.46 (m, 5H), 6.79 (d, $J = 3.7$ Hz, 2H), 6.65 (m, 4H), 3.98 (m, 2H), 2.06–1.25 (m, 20H). ^{13}C NMR (CDCl_3): δ 160.6, 149.5, 142.0, 136.6, 131.2, 130.4, 130.0, 128.1, 117.5, 48.7, 33.2, 31.2, 25.7, 25.1. ESI-MS: m/z 471.29 [M + H] $^+$. λ_{max} (CH_2Cl_2): 460, 350 nm. Anal. calcd for $\text{C}_{29}\text{H}_{34}\text{N}_4\text{O}_2 \cdot 1.25\text{H}_2\text{O}$: C, 70.63; H, 7.46; N, 11.36. Found: C, 70.70; H, 7.79; N, 11.03.

N-Benzyl-1H-pyrrole-2-carboxamide (1c). Trichloroacetylpyrrole (2.0 g, 9.4 mmol) was added to a solution of 1.1 mL of benzylamine and 20 mL of Et_3N . The mixture was stirred at room temperature overnight and became an amber solution. The solvent

was removed on a rotary evaporator. The residue was taken up in 50 mL of CH_2Cl_2 and washed with 2×50 mL of 5% citric acid and 50 mL of brine. The organic layer was dried with Na_2SO_4 and filtered. The solvent was evaporated, and a light brown solid was obtained (1.5 g, 7.4 mmol, 78%). ^1H NMR (500 MHz, CDCl_3): δ 9.43 (s, 1H), 7.37–7.31 (m, 5H), 6.94 (s, 1H), 6.22 (q, $J = 5.8$ Hz, 1H), 5.72 (d, $J = 6.8$ Hz, 1H), 3.93 (m, 1H), 2.02–1.16 (m, 10H). ^{13}C NMR (CDCl_3): δ 161.8, 138.8, 129.0, 127.9, 127.7, 125.9, 122.4, 109.8, 109.8, 43.5. ESI-MS: m/z 193.22 [M + H] $^+$.

[1,1'-Benzylamide-5-phenyl-4,6-dipyrromethane] (2c). To a solution of **1c** (1.5 g, 7.5 mmol) suspended in 30 mL of toluene was added benzaldehyde (0.39 g, 3.7 mmol) and *p*-TSA (~5 mg). The mixture became pale pink upon heating to 94 °C, and a precipitate formed after 2.5 h. The solution was filtered, and the precipitate was washed with 50 mL of toluene (0.40 g, 0.8 mmol, 22%). ^1H NMR (400 MHz, DMSO- d_6): δ 11.35 (s, 2H), 8.43 (q, $J = 5.8$ Hz, 2H), 7.31–7.15 (m, 15H), 6.61 (q, $J = 5.8$ Hz, 2H), 5.58 (q, $J = 5.8$ Hz, 2H), 5.52 (s, 1H), 4.39 (q, $J = 5.8$ Hz, 4H). ^{13}C NMR (DMSO- d_6): δ 161.3, 143.2, 140.7, 137.4, 128.9, 128.8, 127.8, 127.3, 127.0, 126.2, 111.0, 108.5, 43.5, 42.8. ESI-MS: m/z 489.16 [M + H] $^+$, 511.26 [M + Na] $^+$, 527.15 [M + K] $^+$.

[1,1'-Benzylamide-5-phenyl-4,6-dipyrin] (HDADP^{Ph,Bz}). A solution of DDQ (65 mg, 0.29 mmol) in 25 mL of THF was added dropwise to a solution of **2c** (0.10 g, 0.20 mmol) in 25 mL of THF over 15 min. Upon addition, the solution was red and transparent. After 2 h, the reaction was complete by TLC, and the solvent was removed on a rotary evaporator. The residue was purified by flash chromatography on a silica gel column (2% MeOH in CH_2Cl_2), and a red solid was isolated (0.10 g, 0.19 mmol, 99%). ^1H NMR (400 MHz, CDCl_3): δ 7.52–7.28 (m, 15H), 7.12 (s, 2H), 6.81 (d, $J = 4.4$ Hz, 2H), 6.64 (d, $J = 4.4$ Hz, 2H), 4.68 (d, $J = 5.9$ Hz, 2H). ^{13}C NMR (CDCl_3): δ 161.6, 149.0, 142.4, 138.2, 136.5, 131.2, 130.5, 130.0, 129.0, 128.1, 128.0, 127.7, 117.7, 43.8, 29.9. ESI-MS: m/z 487.21 [M + H] $^+$, 509.20 [M + Na] $^+$. λ_{max} (CH_2Cl_2): 458, 340 nm. Anal. calcd for $\text{C}_{31}\text{H}_{26}\text{N}_4\text{O}_2 \cdot 1.75\text{H}_2\text{O}$: C, 71.87; H, 5.74; N, 10.81. Found: C, 72.12; H, 6.12; N, 10.95.

N-Phenyl-1H-pyrrole-2-carboxamide (1d). This compound was prepared according to a literature procedure from freshly distilled aniline (48% yield).²⁷ mp = 152–154 °C (lit: 152–155 °C). ^1H NMR (300 MHz, DMSO- d_6): δ 11.66 (s, 1H), 9.73 (s, 1H), 7.73 (d, $J = 7.7$ Hz, 2H), 7.32 (t, $J = 7.4$ Hz, 2H), 7.02–7.07 (m, 2H), 6.96 (m, sh, 1H), 6.16 (m, sh, 1H).

[1,1'-N-Phenylamide-5-phenyl-4,6-dipyrromethane] (2d). A round-bottomed flask was charged with **1d** (2.5 g, 13 mmol), benzaldehyde (0.71 g, 6.7 mmol), *p*-TSA (~30 mg), and 30 mL of toluene, and the mixture was refluxed for 15 h. The hot slurry was filtered, then washed with hot toluene and benzene to afford **2d** as an off-white powder (2.5 g, 5.5 mmol, 83%). ^1H NMR (400 MHz, DMSO- d_6): δ 11.66 (s, 2H), 9.67 (s, 2H), 7.71 (d, $J = 8.1$ Hz, 4H), 7.29–7.33 (m, 6H), 7.19–7.24 (m, 3H), 7.03 (t, $J = 7.3$ Hz, 2H), 7.00 (t, 2H, $J = 2.93$ Hz), 5.88 (t, $J = 2.9$ Hz, 2H), 5.63 (s, 1H). ^{13}C NMR (DMSO- d_6): δ 159.1, 142.3, 139.4, 137.8, 128.6, 128.2, 128.2, 126.4, 125.5, 122.9, 119.8, 111.6, 108.2, 42.8. ESI-MS: m/z 461.12 [M + H] $^+$, 483.21 [M + Na] $^+$. Anal. calcd for $\text{C}_{29}\text{H}_{24}\text{N}_4\text{O}_2$: C, 75.63; H, 5.25; N, 12.17. Found: C, 75.40; H, 5.63; N, 12.11.

[1,1'-N-Phenylamide-5-phenyl-4,6-dipyrin] (HDADP^{Ph,Ph}). A solution of DDQ (0.17 g, 0.74 mmol) in 5 mL of THF was added dropwise to a solution of **2d** (0.31 g, 0.67 mmol) in 25 mL of THF over 15 min. Upon addition, the solution became dark orange. The

(27) La Regina, G.; Silvestri, R.; Artico, M.; Lavecchia, A.; Novellino, E.; Befani, O.; Turini, P.; Agostinelli, E. *J. Med. Chem.* **2007**, *50*, 922–931.

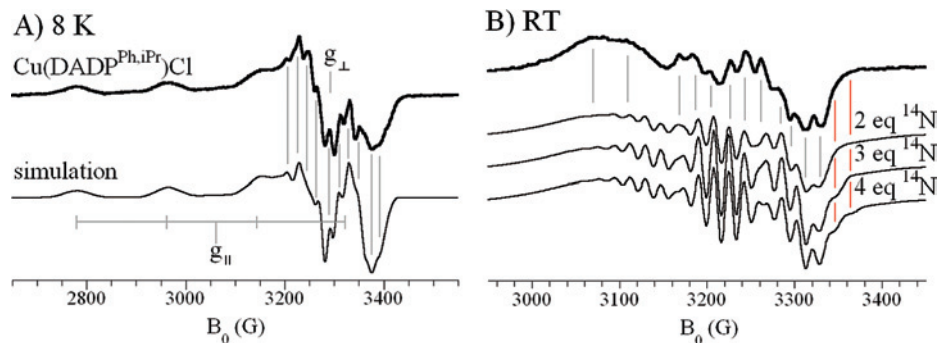


Figure 1. X-band EPR spectra (bold lines), and relevant simulations (thin lines), of Cu(DADP^{Ph,iPr})Cl in frozen solution (A) and in fluid solution (B). The gray vertical lines are included to aid in comparison of the visible features in the experimental spectra with features in the simulations; the red vertical lines in B represent the additional features anticipated when more than two equivalent ¹⁴N atoms are coordinated, as described in the text.

reaction was continued for 3 h, and the precipitate was collected and washed with 10 mL of THF followed by ethyl ether (2 × 10 mL) to afford the product as a red powder (0.15 g, 0.32 mmol, 47%). ¹H NMR (400 MHz, CDCl₃): δ 10.46 (s, 2H), 7.85 (d, *J* = 8.6 Hz, 4H), 7.55–7.66 (m, 5H), 7.37 (t, *J* = 8.1 Hz, 4H), 7.12–7.16 (m, 4H), 6.70 (d, *J* = 4.4 Hz, 2H). ¹³C NMR (CDCl₃): δ 159.2, 149.4, 145.3, 140.9, 138.4, 135.7, 130.6, 130.2, 129.9, 128.6, 128.0, 123.8, 119.8, 118.9. ESI-MS: *m/z* 459.18 [M + H]⁺.

[1,1'-Isopropylamide-5-phenyl-4,6-dipyrrinato]CuCl [Cu(DADP^{Ph,iPr})Cl]. A solution of CuCl₂·2H₂O (14 mg, 0.08 mmol) in 3.0 mL of CH₃OH was added to a solution of DADP^{Ph,iPr} (20 mg, 0.05 mmol) in 3.0 mL of CHCl₃. Upon addition, the solution turned from red to a magenta color. Triethylamine (Et₃N, 0.20 mL) was added, and the solution became dark purple. The solution was evaporated, and the residue was taken up in CH₂Cl₂. The residue was washed with 10 mL of ddH₂O, and the organic layer was dried, giving a dark purple precipitate (32 mg, 0.07 mmol, 99%). ESI-MS: *m/z* 451.22 [M]⁺. λ_{max} (15% CH₃OH/CH₂Cl₂): 546 (25000), 362 (14000). Anal. calcd for C₂₃H₂₅N₄CuO₂: C, 56.55; H, 5.16; N, 11.47. Found: C, 56.94; H, 5.20; N, 11.23.

[1,1'-Isopropylamide-5-phenyl-4,6-dipyrrinato]Ni [Ni(DADP^{Ph,iPr})]. NiCl₂ (5.4 mg, 0.04 mmol) was suspended in 3.0 mL of CH₃OH and was added to a solution of DADP^{Ph,iPr} (16 mg, 0.04 mmol) in 3.0 mL of CHCl₃. Upon vigorous stirring, the solution turned from red to a magenta color. Et₃N (0.20 mL) was added, and the solution became brown. The solution was evaporated, and the residue was taken up in CH₂Cl₂ and 0.20 mL of Et₃N. The solution was diffused with hexanes and then allowed to slowly evaporate. The residue was washed with chloroform, and red-green dichroic crystals of the CH₂Cl₂ solvate were collected on a glass frit (12 mg, 0.03 mmol, 73%). ¹H NMR (500 MHz, DMSO-*d*₆): δ 10.46 (s, br, 2H), 7.60 (t, 1H, *J* = 7.4 Hz), 7.54 (t, *J* = 7.5 Hz, 2H), 7.46 (d, *J* = 7.5 Hz, 2H), 6.72 (d, *J* = 4.0 Hz, 1H), 6.64 (d, *J* = 4.6 Hz, 1H), 6.49 (d, *J* = 4.0 Hz, 1H), 6.35 (d, *J* = 4.6 Hz, 1H), 3.92–3.97 (m, 1H), 3.81–3.86 (m, 1H), 1.21 (d, *J* = 6.3 Hz, 6H), 0.94 (d, *J* = 6.9 Hz, 6H). ESI-MS: *m/z* 447.17 [M + H]⁺. λ_{max} (15% CH₃OH /CH₂Cl₂): 504 (26000), 476 (15000), 362 (11000). Anal. calcd for C₂₃H₂₄N₄NiO₂·0.5H₂O: C, 60.56; H, 5.52; N, 12.28. Found: C, 60.23; H, 5.62; N, 11.91.

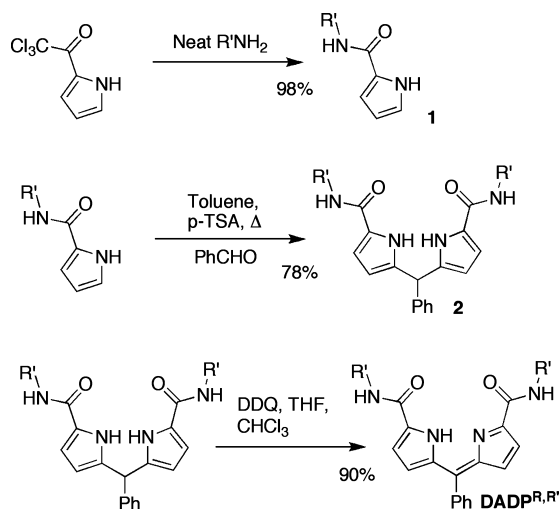
1,1'-Isopropylamide-5-phenyl-4,6-dipyrrinium Bromide (H₂-DADP^{Ph,iPr}Br). (H₂DADP^{Ph,iPr}Br). HDADP^{Ph,iPr} (16 mg, 0.04 mmol) was added to a solution of concentrated HBr (4.7 μL, 0.04 mmol) in 5.0 mL of CHCl₃. After 20 min, the reaction mixture was filtered and the solvent evaporated to afford the product in quantitative yield. X-ray-quality single crystals of H₂DADP^{Ph,iPr}Br·3CHCl₃·H₂O grew from a concentrated CHCl₃ solution at -20 °C.

Copper-Mediated Oxidation of 2a. 1,1'-Isopropylamide-5-phenyl-4,6-dipyrromethane (**2a**) (0.40 mM) and CuCl₂·2H₂O (0.33

mM) solutions were prepared in HPLC-grade THF (Fisher Scientific) containing 0.80% (v/v) Et₃N. Both solutions were subjected to three freeze–pump–thaw cycles under a N₂ atmosphere and then transferred to an inert atmosphere (N₂) glovebox. *Air-free method:* In the glovebox, a septum-capped quartz cuvette was charged with 1.5 mL of the **2a** stock solution and 1.8 mL of the CuCl₂·2H₂O stock solution to give a final concentration of 0.18 mM in each component. UV–visible spectra were obtained at 5 min intervals over the course of 3 h. *Aerated method:* This method was identical to the airless method except that, following the initial scan, air was bubbled through the solution with a Pasteur pipet for 2 min. The cuvette was then resealed, and absorbance spectra were obtained every 5 min for 3 h. For aerated reactions involving only **2a** or only CuCl₂·2H₂O, THF with 0.80% Et₃N was substituted for the volume of the omitted reagent. In an attempt to ascertain the identity of the reaction mixture, the aerated reaction was continued for 24 h. UV–visible spectroscopy confirmed that the spectrum after 24 h was essentially identical to the final spectrum after 3 h. The reaction was concentrated to about 2 mL under reduced pressure and then analyzed by mass spectrometry. ESI-MS, mass calcd for Cu(DADP^{Ph,iPr}): *m/z* = 451.12 [M]⁺. Found: *m/z* = 452.18 [M + H]⁺.

Single Crystal X-Ray Crystallographic Studies. Single crystals of each compound suitable for X-ray diffraction structural determination were mounted on nylon loops with Paratone oil and were cooled in a nitrogen stream on the diffractometer. Data were collected on either a Bruker AXS or a Bruker P4 diffractometer, each equipped with area detectors. Peak integrations were performed with the Siemens SAINT software package. Absorption corrections were applied using the program SADABS. Space group determinations were performed by the program XPREP. The structures were solved and refined with the SHELXTL software package (Sheldrick, G. M. *SHELXTL vers. 5.1 Software Reference Manual*; Bruker AXS: Madison, WI, 1997). All structures were solved by direct methods; all hydrogen atoms were placed at calculated positions and treated with a riding model, and all non-hydrogen atoms were refined anisotropically unless otherwise noted.

EPR Spectroscopy. X-band EPR spectra were recorded with a Bruker EMX EPR spectrometer on degassed 50 μM 80/20 CH₂Cl₂/toluene solutions of Cu(DADP^{Ph,iPr})Cl. Low-temperature spectra were obtained using an Oxford ESR900 liquid helium cryostat. To facilitate direct comparison of the fluid and frozen solution spectra, both sets of data were acquired with the cryostat in place, keeping the microwave frequency nearly constant. The spectra in Figure 1 represent the average of 16 scans each. Other conditions are as follows: (room temperature) ν_{MW} = 9.372 GHz (20 mW), 6 G field modulation (100 kHz), receiver gain = 50 000, time constant/conversion time = 82 ms; (8 K) ν_{MW} = 9.385 GHz (20 μW), 6 G field modulation (100 kHz), receiver gain = 50 000, time constant/

Scheme 1. Synthesis of DADP^{R,R'} Ligands Starting with Trichloroacetylpyrrole^a

^a The yields shown are for R = Ph and R' = *i*Pr; however, it should be noted that, although the yields of these reactions are generally high, they may vary with different R and R' substituents.

conversion time = 82 ms. Spectra were simulated using the program QPOW (QPOW is available upon request from Prof. Joshua Telser, Roosevelt University, Chicago, IL). The low-temperature spectrum in Figure 1A was simulated by adjusting hyperfine couplings and *g* values to match peak positions and then increasing the EPR line width, ultimately to 10 (*g*_⊥) or 15 MHz (*g*_∥), without further adjustment of the *g* and *A* values. An isotropic coupling of 46 MHz to two equivalent ¹⁴N's is also included in the low-temperature simulation, as discussed below. The average *g* and *A* values obtained from the low-temperature simulation were then held fixed to generate the room temperature simulations in Figure 1B. The final simulations include weighted contributions from both ⁶³Cu and ⁶⁵Cu, and correlated *m*_l and frequency-dependent contributions to the observed line width,²⁸ totaling less than 20% of the overall EPR line width; the same line width parameters were used for both simulations.

Results and Discussion

The synthesis of diamidodipyrrens is quite facile, high-yielding, and versatile; indeed, in our hands, the synthetic chemistry is more straightforward than that of the parent α -unsubstituted dipyrrens. Adapted from existing reports of diamidodipyrromethanes,^{22,23} the synthesis of diamidodipyrrens (Scheme 1) begins with the amination of trichloroacetylpyrrole to yield a pyrrolamide (**1**). The acid-catalyzed (*p*-TSA), heat-driven condensation of benzaldehyde with the pyrrolamide in toluene generates the dipyrromethane (**2**) as an insoluble precipitate. The dipyrromethane is then oxidized with DDQ to give the expected dipyrin product as a bright orange solid. Unlike many previously reported α -unsubstituted dipyrrens,^{9,11} diamidodipyrin ligands can be chromatographed on silica and isolated in high yields after oxidation from the corresponding diamidodipyrromethane (typically >90% for the oxidation step) with relative ease. The synthesis described is relatively general, and the R and R' substituents of the diamidodipyrrens can be modified

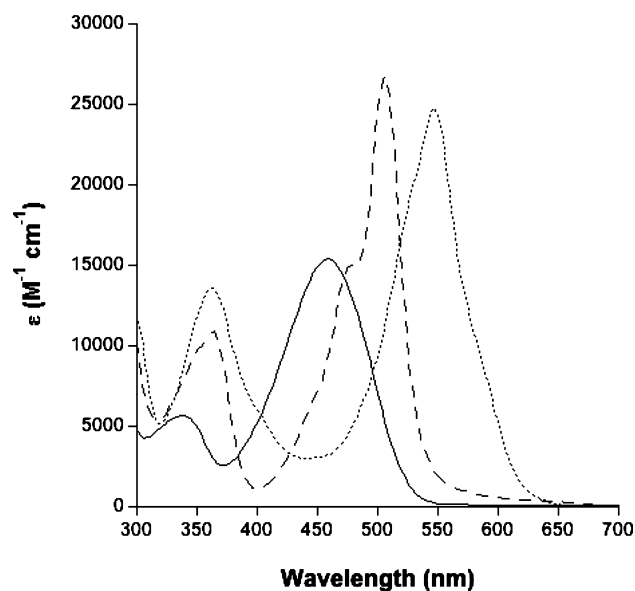


Figure 2. Electronic absorbance spectrum in 15% CH₃OH/CH₂Cl₂ of DADP^{Ph,*i*Pr} (—), Cu[DADP^{Ph,*i*Pr}]Cl (····), and Ni[DADP^{Ph,*i*Pr}] (---).

without significant changes to the approach outlined in Scheme 1 (diamidodipyrin ligands are abbreviated as DADP^{R,R'}). In this initial study, ligands containing R = Ph and R' = *i*Pr, Cy, Ph, and Bn were readily prepared. The versatile synthesis of these ligands is one attractive feature for their use in exploring new metal complexes.

The diamidodipyrin ligands are found to readily form metal complexes under mild conditions. An appropriate metal salt in CH₃OH is added to the ligand dissolved in CHCl₃ at room temperature. The reaction can be visually monitored by its intense color changes. For example, when adding either CuCl₂·2H₂O or NiCl₂ to a solution of DADP^{Ph,*i*Pr}, an immediate color change from red to magenta is observed. The addition of a base causes the solution to become dark purple and red-brown for the Cu²⁺ and Ni²⁺ complexes, respectively. The addition of a base is necessary as the reaction in the absence of a base results in the isolation of the ligand as a hydrogen-bonded, protonated dimer (vide infra). Electrospray ionization mass spectrometry (ESI-MS) analysis reveal an [M]⁺ (*m/z* 451.22) and [M + H]⁺ (*m/z* 447.21) peak for Cu(DADP^{Ph,*i*Pr})Cl and Ni(DADP^{Ph,*i*Pr}), respectively.

The absorbance spectra of both complexes and DADP^{Ph,*i*Pr} are shown in Figure 2. Cu(DADP^{Ph,*i*Pr})Cl has a maximum absorbance at 546 nm ($\epsilon = 25\,000\text{ M}^{-1}\text{ cm}^{-1}$), while Ni(DADP^{Ph,*i*Pr}) has a maximum absorbance at 506 nm ($\epsilon = 26\,000\text{ M}^{-1}\text{ cm}^{-1}$). The complexes are significantly red-shifted relative to the DADP^{Ph,*i*Pr} ligand, which has a maximum absorbance at 458 nm ($\epsilon = 15\,000\text{ M}^{-1}\text{ cm}^{-1}$). Due to the extended conjugation of the dipyrin unit with the carbonyl groups in the DADP^{Ph,*i*Pr} ligand, the spectra of the complexes reported here are also red-shifted relative to the α -unsubstituted dipyrinato complexes,^{14,29,30} which typically display a maximum absorbance at $\leq 500\text{ nm}$.

(29) Brückner, C.; Karunaratne, V.; Rettig, S. J.; Dolphin, D. *Can. J. Chem.* **1996**, *74*, 2182–2193.

(30) Halper, S. R.; Cohen, S. M. *Chem.—Eur. J.* **2003**, *9*, 4661–4669.

(28) Froncisz, W.; Hyde, J. S. *J. Chem. Phys.* **1980**, *73*, 3123–3131.

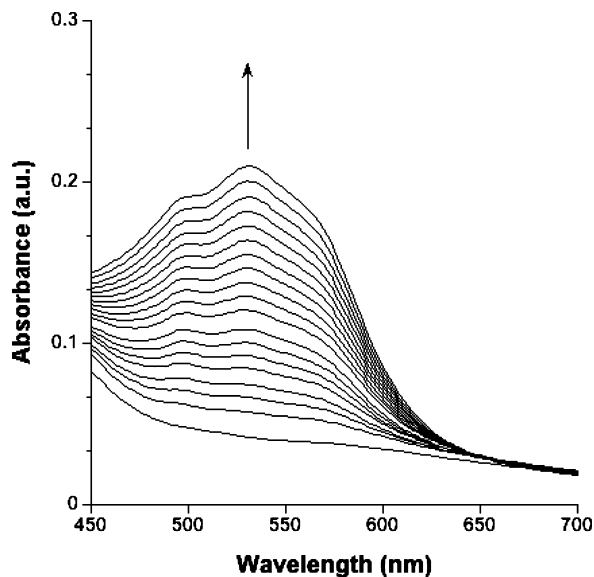


Figure 3. Time-elased visible absorption spectroscopy of the reaction of 0.18 mM **2a** and 0.18 mM $\text{CuCl}_2 \cdot 2\text{H}_2\text{O}$ in THF (0.8% by vol Et_3N) in the presence of O_2 . The spectrum was monitored at 5 min intervals for 3 h (spectra shown are in 10 min intervals).

Copper-Mediated Oxidation of **2a.** While preparing solutions for electronic spectroscopic studies, we noticed that the reaction of 1,1'-isopropylamide-5-phenyl-4,6-dipyrrromethane (**2a**) and CuCl_2 in the presence of air and a base (Et_3N) produced a red solution. A similar color change did not occur when NiCl_2 was used as a metal ion source. We interpreted this color change as an indication of the copper-mediated oxidation of the dipyrromethane to the dipyririn, presumably followed by the formation of a complex with Cu^{2+} . It has been noted in the literature that solutions of dipyrromethanes oxidize over time to form dipyririns; this has also been noted for diamidodipyrromethanes as well.²² The oxidation of diiminodipyrromethane complexes of group 10 metals has also been reported.³ In an attempt to ascertain the dependence of this reaction on the various reagents, we monitored the reaction by UV–visible absorbance spectroscopy.

As shown in Figure 3, a broad visible band centered at 530 nm increased in intensity over time when the reaction was exposed to the air. This band, which was responsible for the red color, was not present when air was excluded from the reaction. Also, there was no color change indicative of oxidation when the experiment was performed with the omission of either **2a** or CuCl_2 in aerated solutions containing Et_3N (data not shown). These results show that both CuCl_2 and oxygen were required for the rapid oxidation of **2a**. The formation of the resulting $\text{Cu}[\text{DADP}^{\text{Ph},i\text{Pr}}]\text{Cl}$ complex was confirmed by ESI-MS on an aliquot of the reaction mixture, as well as the growth and X-ray structure determination of single crystals of $\text{Cu}[\text{DADP}^{\text{Ph},i\text{Pr}}]\text{Cl}$ produced directly from the solution.

Structure of $\text{HDADP}^{\text{Ph},i\text{Pr}}$. A weakly diffracting, orange plate of the free-base $\text{HDADP}^{\text{Ph},i\text{Pr}}$ crystallized from a chloroform solution by vapor diffusion with pentane (Table 1). The crystal formed in the monoclinic, $P2_1/c$, space group. The asymmetric unit of the solvent-free crystal included two dipyririn molecules. Each independent molecule included a

disordered isopropyl group. All hydrogen atoms were located in a difference map. The positions of the N-amide and pyrrolic hydrogen atoms were allowed to refine freely. One of the two molecules is displayed in Figure 4. The most striking feature of the structure is that the deprotonated pyrrolic nitrogen atoms (N3) accept intramolecular hydrogen bonds from both the protonated pyrrolic hydrogen atom and from the proximal N-amide hydrogen atom (the hydrogen atoms bonded to N2 and N4 in the figure). The resulting geometric arrangement, if it persists in solution, may predispose the ligand toward a NNNO coordination mode (vide infra). The carbonyl oxygen atom directed toward the core of the molecule does not appear to be involved in intramolecular hydrogen bonding. The molecules form a hydrogen-bonded chain through intermolecular interactions of the outwardly directed C–O and N–H groups, as shown in Figure 4.

Structure of $\text{H}_2\text{DADP}^{\text{Ph},i\text{Pr}}\text{Br}$. Crystals of $\text{H}_2\text{DADP}^{\text{Ph},i\text{Pr}}\text{Br} \cdot 3\text{CHCl}_3 \cdot \text{H}_2\text{O}$ grew upon cooling a concentrated solution of $\text{H}_2\text{DADP}^{\text{Ph},i\text{Pr}}\text{Br}$ in chloroform to -20°C (Table 1). The red needles crystallized in the monoclinic space group $P2_1/n$. The asymmetric unit included two independent $[\text{H}_2\text{DADP}^{\text{Ph},i\text{Pr}}]^+$ cations and two Br^- anions, as well as six CHCl_3 and two H_2O solvent molecules. The cations are arranged in a hydrogen-bonded dimer through cooperative hydrogen bonding of the pyrrole hydrogen atoms of each monomer with the carbonyl oxygen atoms of the other monomer as shown in Figure 5. We have observed similar cooperative hydrogen bonding in other $[\text{H}_2\text{DADP}^{\text{Ph},i\text{Pr}}]^+$ salts (data not shown), which suggests the persistence of this motif. This pattern of cooperative hydrogen bonding has also been observed for a related dipyrromethane compound, 5,5'-diformyl-2,2'-diphenyldipyrromethane.³¹

Structure of $\text{M}(\text{DADP}^{\text{Ph},i\text{Pr}})$ Complexes. Single crystals of $\text{Cu}(\text{DADP}^{\text{Ph},i\text{Pr}})\text{Cl}$ and $\text{Ni}(\text{DADP}^{\text{Ph},i\text{Pr}})$ were obtained, and their structures were determined by X-ray diffraction (Figure 6, Table 1). Red plates of $\text{Cu}(\text{DADP}^{\text{Ph},i\text{Pr}})\text{Cl}$ crystallized in the orthorhombic space group $P2_12_12_1$ with two independent complexes in the asymmetric unit and two CH_3OH and one H_2O solvent molecule. The copper center has a square-pyramidal coordination geometry bound to a single $\text{DADP}^{\text{Ph},i\text{Pr}}$ ligand via two pyrrolic nitrogen atoms and two amide oxygen atoms, forming a NNNO donor set. This coordination mode is very reminiscent of the dialkyltin complexes formed with saturated 1,9-diacetyldipyrromethanes reported by Lindsey and co-workers.³² The apical position in $\text{Cu}(\text{DADP}^{\text{Ph},i\text{Pr}})\text{Cl}$ is occupied by the chloride ligand. The Cu–N distances are 1.911(3) and 1.917(3) Å and the Cu–O distances are 2.031(2) and 2.116(3) Å. Cu^{2+} complexes of α -unsubstituted dipyririns have average Cu–N bond distances of 1.953(17) Å, while Cu^{2+} – O_{amide} distances average 2.06(17) Å.³³ Intermolecular hydrogen bonding is observed between

(31) Love, J. B.; Blake, A. J.; Wilson, C.; Reid, S. D.; Novak, A.; Hitchcock, P. B. *Chem. Commun.* **2003**, 1682–1683.

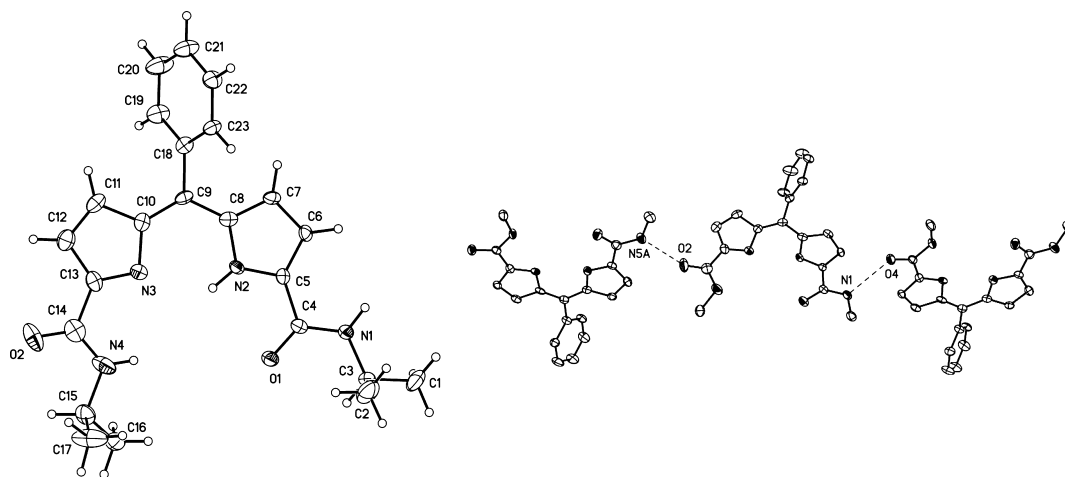
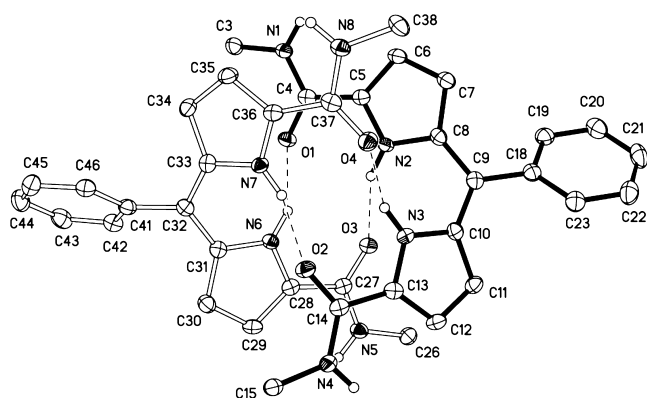
(32) Tamaru, S.; Yu, L. H.; Youngblood, W. J.; Muthukumar, K.; Taniguchi, M.; Lindsey, J. S. *J. Org. Chem.* **2004**, *69*, 765–777.

(33) Allen, F. H. *Acta Crystallogr.* **2002**, *B58*, 380–388.

Table 1. Crystal Data and Data Collection Parameters for HDADP^{Ph,iPr}, H₂DADP^{Ph,iPr}Br·3CHCl₃·H₂O, Cu(DADP^{Ph,iPr})Cl, and Ni(DADP^{Ph,iPr})

	HDADP ^{Ph,iPr}	H ₂ DADP ^{Ph,iPr} Br	Cu(DADP ^{Ph,iPr})Cl	Ni(DADP ^{Ph,iPr})
empirical formula	C ₂₃ H ₂₆ N ₄ O ₂	C ₂₃ H ₂₇ N ₄ O ₂ Br·3CHCl ₃ ·H ₂ O	C ₂₄ H ₃₀ CuN ₄ O _{2.5} Cl	C ₂₄ H ₂₆ N ₄ NiO ₂ Cl ₂
cryst syst	monoclinic	monoclinic	orthorhombic	monoclinic
space group	<i>P</i> 2 ₁ / <i>c</i>	<i>P</i> 2 ₁ / <i>n</i>	<i>P</i> 2 ₁ 2 ₁ 2 ₁	<i>P</i> 2 ₁ / <i>n</i>
unit cell dimensions	<i>a</i> = 15.7923(19) Å <i>b</i> = 13.3540(17) Å <i>c</i> = 21.442(3) Å α = 90° β = 106.781(2)° γ = 90°	<i>a</i> = 13.987(3) Å <i>b</i> = 20.692(5) Å <i>c</i> = 25.444(6) Å α = 90° β = 94.605(5)° γ = 90°	<i>a</i> = 11.850(4) Å <i>b</i> = 16.419(5) Å <i>c</i> = 25.676(8) Å α = 90° β = 90° γ = 90°	<i>a</i> = 8.5116(6) Å <i>b</i> = 15.8157(11) Å <i>c</i> = 17.9622(12) Å α = 90° β = 90.2120(10)° γ = 90°
volume, <i>Z</i>	4329.4(9) Å ³ , 8	7340(3) Å ³ , 8	4996(3) Å ³ , 8	2418.0(3) Å ³ , 4
crystal size	0.34 × 0.25 × 0.07 Å ³	0.41 × 0.22 × 0.19 Å ³	0.15 × 0.12 × 0.08 Å ³	0.29 × 0.26 × 0.11 Å ³
temp (K)	100(2)	100(2)	208(2)	100(2)
reflns collected	39697	93094	19863	12149
independent reflns	7917 [<i>R</i> (int) = 0.1413]	14795 [<i>R</i> (int) = 0.0545]	9634 [<i>R</i> (int) = 0.0476]	4719 [<i>R</i> (int) = 0.0380]
data/restraints/params	7917/3/583	14795/6/805	9634/3/621	4719/0/309
goodness of fit on <i>F</i> ²	1.020	1.018	1.024	1.059
final <i>R</i> indices <i>I</i> > 2σ(<i>I</i>)	<i>R</i> ₁ = 0.0942 <i>wR</i> ₂ = 0.1386	<i>R</i> ₁ = 0.0406 <i>wR</i> ₂ = 0.0898	<i>R</i> ₁ = 0.0445 <i>wR</i> ₂ = 0.0985	<i>R</i> ₁ = 0.0425 <i>wR</i> ₂ = 0.0863
<i>R</i> indices (all data)	<i>R</i> ₁ = 0.1806 <i>wR</i> ₂ = 0.1660	<i>R</i> ₁ = 0.0594 <i>wR</i> ₂ = 0.0987	<i>R</i> ₁ = 0.0605 <i>wR</i> ₂ = 0.1078	<i>R</i> ₁ = 0.0691 <i>wR</i> ₂ = 0.0955

$$^a R_1 = \frac{\sum |F_o| - |F_c|}{\sum |F_o|}, R_2 = \frac{\{\sum [w(F_o^2 - F_c^2)^2] / \sum [wF_o^4]\}^{1/2}}$$

**Figure 4.** A drawing of one of the two independent molecules in the crystal structure of HDADP^{Ph,iPr} (left). Atoms are shown with 50% thermal contours. The second molecule has a similar geometry. For clarity, only one position of the disordered isopropyl group is shown. A view showing the connectivity of a hydrogen-bonded chain in HDADP^{Ph,iPr} is also given (right). For clarity, only *ipso*-isopropyl carbon atoms are shown, and hydrogen atoms are omitted.**Figure 5.** A drawing with partial naming scheme of the hydrogen-bonded dimer in H₂DADP^{Ph,iPr}Br·3CHCl₃·H₂O. Atoms are drawn with 50% thermal contours. For clarity, only pyrrolic and amide hydrogen atoms and *ipso*-carbon atoms of the isopropyl groups are shown.

the N–H amide groups and chloride ligands of an adjacent complex.

Red blocks of Ni(DADP^{Ph,iPr}) were crystallized in the monoclinic space group *P*2₁/*n* with one complex in the asymmetric unit and one disordered CH₂Cl₂ solvent molecule

(Figure 6, Table 1). Interestingly, Ni(DADP^{Ph,iPr}) shows a NNNO coordination set with a square-planar coordination geometry. The Ni–N bond lengths in Ni(DADP^{Ph,iPr}) are all shorter than those found in Cu(DADP^{Ph,iPr})Cl, as expected. The Ni–N_{pyrrole} bond lengths are 1.808(2) and 1.824(2) Å, while the Ni–N_{amide} and Ni–O lengths are 1.908(2) and 1.9132(18) Å, respectively. These distances may be compared with the average bond lengths of 1.91(4) Å (Ni–N_{pyrrole}), 1.91(9) Å (Ni–N_{amide}), and 2.05(11) Å (Ni–O_{amide}). The sum of the angles about the nickel atom is 360°, with N_{pyrrole}–Ni–N_{pyrrole}, N_{pyrrole}–Ni–N_{amide}, N_{pyrrole}–Ni–O, and N_{amide}–Ni–O angles of 88.54(10)°, 84.31(10)°, 83.92(9)°, and 103.22(9)°. ³³ Intermolecular hydrogen bonding is observed between the N–H amide group and the amide oxygen of an adjacent molecule. A similar complex, generated via oxygen activation of a Ni²⁺ diiminodipyrinato complex to obtain a Ni²⁺ iminocarboxylatodipyrinato complex, has also been described.³ That complex had an identical NNNO donor set to Ni(DADP^{Ph,iPr}) and quite similar metrics, with Ni–N_{pyrrole} bond lengths of 1.829 Å and 1.845 Å, and Ni–N_{imine} and Ni–O_{carboxylate} bond

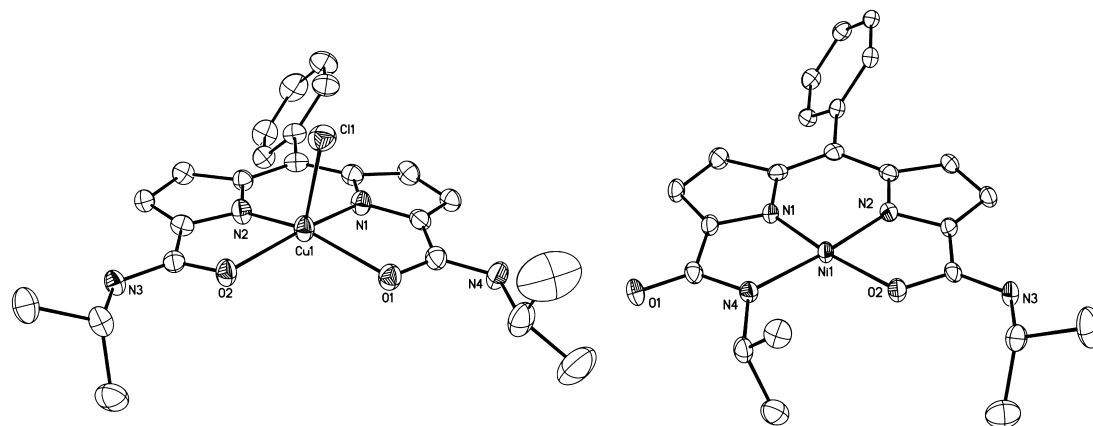


Figure 6. Structures of Cu(DADP^{Ph,iPr})Cl (left) and Ni(DADP^{Ph,iPr}) (right). The structures are drawn with 50% thermal contours.

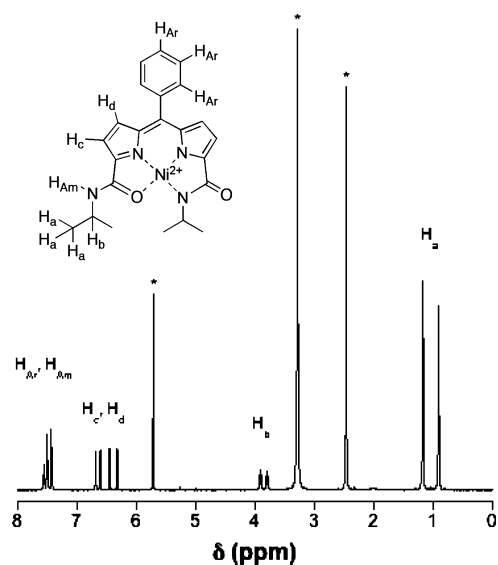


Figure 7. ¹H NMR spectrum of Ni(DADP^{Ph,iPr})·CH₂Cl₂ in a DMSO-*d*₆ solution clearly showing that the asymmetric NNNO mode of binding persists in solution. Ligand resonances are labeled according to the inset chemical diagram, and solvent peaks are labeled with asterisks.

lengths of 1.970 Å and 1.988 Å, as well as similar bond angles about the Ni²⁺.

The asymmetric NNNO binding mode of Ni(DADP^{Ph,iPr}) was confirmed by the ¹H NMR spectrum of dissolved crystals of Ni(DADP^{Ph,iPr})·CH₂Cl₂. As shown in Figure 7, the ligand resonances are split into two sets of peaks of equal intensity, indicative of the asymmetric binding mode of the chelator. For example, the resonances associated with the isopropyl substituents show as two doublets at 0.94 and 1.21 ppm for the methyl groups, and the ipso protons show up as two separate multiplets at 3.84 and 3.95 ppm. The ¹H NMR data unambiguously show that the Ni²⁺ coordination environment observed in the solid state is preserved in solution.

EPR studies of Cu(DADP^{Ph,iPr})Cl also suggest that the coordination mode observed in the solid state is maintained in fluid solution. The axial spectrum observed in frozen solution (bold line in Figure 1A) is similar in appearance to that of axially coordinated Cu(II) porphyrins,^{34–37} with three

of the four ^{63,65}Cu hyperfine lines visibly resolved at $g_{\parallel} = 2.194$ ($A_{\parallel}({}^{63}\text{Cu}) = 555$ MHz) and the fourth overlapping the rich hyperfine structure at $g_{\perp} = 2.052$ ($A_{\perp}({}^{63}\text{Cu}) = 52$ MHz). The values of g_{\parallel} and $A_{\parallel}({}^{63}\text{Cu})$ indicate that the Cu(II) ion remains five-coordinate in solution.^{38,39} In order to adequately simulate the low-temperature spectrum, it was necessary to include at least two equivalent ¹⁴N's in order to match the experimental line shape. The Cu–N hyperfine coupling was assumed to be isotropic, consistent with previous studies of Cu(II) porphyrins,^{34–37} and set to the highest-field splitting observed in the room-temperature spectrum (47 MHz, Figure 1B). The similarity of $A_{\perp}({}^{63,65}\text{Cu})$ and $A_{\perp}({}^{14}\text{N})$, together with a lack of resolution at the high-field edge of the spectrum, makes it impossible to define the number of N donors from the low-temperature spectrum. However, the low-temperature spectrum provides a framework for analysis of the isotropic spectrum, by fixing the values of g_{avg} and $A_{\text{avg}}({}^{63}\text{Cu})$ at 2.100 and 220 MHz, respectively. The room-temperature, fluid solution spectrum (Figure 1B) shows a series of progressively sharper features whose positions are well predicted using these values. On the assumption that an equatorial Cu–N_{pyrrole} hyperfine coupling will be approximately the same as an equatorial Cu–N_{amide} coupling in this complex,³⁶ the only resolvable difference that is predicted, on going from two to three to four equivalent N donors, is the number of lines that will be observed at the high-field edge of the spectrum (red vertical lines in Figure 1B). The experimental spectrum gives no evidence of additional lines beyond those predicted in the 2N simulation, suggesting that the symmetric 2N2O coordination mode, observed in the solid state, is also the preferred geometry for this Cu²⁺ complex in fluid solution.

Conclusion

The facile, high-yielding syntheses of DADP^{R,R'} make these ligands superb candidates for exploring the coordination chemistry of a new class of nonporphyrinic pyrrole-derived

(34) Alston, K.; Storm, C. B. *Biochemistry* **1979**, *18*, 4292–4300.

(35) Brown, T. G.; Hoffman, B. M. *Mol. Phys.* **1980**, *39*, 1073–1109.

(36) Iwaizumi, M.; Kudo, T.; Kita, S. *Inorg. Chem.* **1986**, *25*, 1546–1550.

(37) Iwaizumi, M.; Ohba, Y.; Iida, H.; Hirayama, M. *Inorg. Chim. Acta* **1984**, *82*, 47–52.

(38) Bubacco, L.; van Gastel, M.; Groenen, E. J. J.; Vijgenboom, E.; Canters, G. W. *J. Biol. Chem.* **2003**, *278*, 7381–7389.

(39) Peisach, J.; Blumberg, W. E. *Arch. Biochem. Biophys.* **1974**, *165*, 691–708.

Diamidodipyrins

ligands. Acid salts of these ligands show a strong propensity to form hydrogen-bonded dimers in the solid state. The ligands are readily derivatized with a variety of substituents, both at the amide groups and at the meso position of the dipyrin, and show the ability to employ different donor atoms with different metal ions. We have also found that Cu^{2+} and O_2 can oxidize diamidodipyrromethanes in situ to form the corresponding $\text{DADP}^{\text{R,R}'}$ complexes.³ These new dipyrinato complexes may have potential in a variety of applications, and ongoing studies to investigate their metal complexes with transition and group 13 ions are underway.

Acknowledgment. We thank Dr. A. G. DiPasquale and Prof. A. L. Rheingold for help with X-ray analyses and Dr.

Y. Su for performing the mass spectrometry experiments. This work was supported by U.C.S.D., the donors of the ACS-PRF, and the NSF (CHE-0546531). The EPR spectrometer was purchased with funds provided by the NSF (CHE-0216277).

Supporting Information Available: Complete crystallographic details (CIF file). This material is available free of charge via the Internet at <http://pubs.acs.org>. X-ray crystallographic files in CIF format are also available free of charge via the Internet at <http://www.ccdc.cam.ac.uk>. Refer to CCDC reference numbers 673246, 673247, 692209, and 692210.

IC8011876